FACULTAD DE MEDICINA
UNIVERSIDAD DE CANTABRIA

GRADO EN MEDICINA

TRABAJO FIN DE GRADO

Encapsulación de fármacos antitumorales y su liberación en células modelo de Cáncer de Cabeza y Cuello.

Encapsulation of anti-tumor drugs and their release in model cells of head and neck cancer.

Autor:
Faunier Hernán Ríos Jaramillo

Directoras:
Nerea Iturrioz Rodriguez
Mónica López Fanarraga

Santander, Junio 2020

INDEX

Resumen

Los tumores de cabeza y cuello corresponden a un grupo diverso de enfermedades, siendo el tipo histológico más representativo el carcinoma epidermoide de laringe, faringe y cavidad oral. Constituyen una patología altamente desafiante, considerando la complejidad anatómica de la región cérvico-facial y las repercusiones funcionales y estéticas que pueden derivarse tanto de la enfermedad como de su tratamiento. Por este último motivo se considera urgente la búsqueda de nuevos tratamientos que sean menos agresivos, más específicos y con menos efectos secundarios. En este trabajo de fin de grado experimental se han diseñado unas nanopartículas de sílice como trasportadores de un fármaco antitumoral (Taxol) que, para garantizar su especificidad frente a células modelo de CCC se han funcionalizado con una proteína quimera recombinante que contiene el dominio de interacción de la toxina Shiga, cuya diana molecular es el Globotriaosylceramida (Gb3), un glucoesfingolípido sobreexpresado en la superficie de las células del CCC. Este estudio emplea la nanotecnología en el diseño y ensamblaje de un sistema para encapsular quimiotreapia y liberarla de forma controlada en el interior de las células de CCC empleando el receptor Gb3 y la toxina Shiga como ligando de las NPs.

Palabras clave:

Nanomedicina, Nanopartículas, Cáncer, Globotriaosylceramida (Gb3).

Abstract

Head and neck cancers correspond to a diverse group of diseases, in which the most representative histological type is squamous cell carcinoma of the larynx, pharynx and oral cavity. They constitute a highly challenging pathology, considering the anatomical complexity of the cervico-facial region and the functional and aesthetic repercussions that can be derived from both the disease and its treatment. For this last reason, the search for new treatments that are less aggressive, more specific and with fewer side effects is considered urgent. In this final degree project, we have worked with silica nanoparticles used as a transporter of an antitumoral drug (Taxol) and to guarantee their specificity against model HNC cells, these particles have been functionalized with a recombinant chimera protein that contains the interaction domain of the Shiga toxin, whose molecular target is Globotriaosylceramide (Gb3), a glycosphingolipid overexpressed on the surface of HNC cells. This study uses nanotechnology in the design and assembly of a nanosystem to encapsulate chemotherapy and release it in a controlled way inside the HNC cells using the Gb3 receptor and the Shiga toxin as a ligand for the NPs.

Keywords:

Nanomedicine, Nanoparticles, Cancer, Globotriaosylceramide (Gb3).

INTRODUCTION

Head and Neck Cancer

The facial cervical region includes the extra-cranial head and neck, with its lower limit corresponding to the clavicles, shoulder blades and first rib. Its anatomy is highly complex, as it contains multiple vital structures in a relatively small space: large vessels that supply the brain, spinal cord, cranial nerves, airway and upper digestive tract, as well as the sense organs as it is illustrated in Image 1.

Of the multiple pathologies that can affect this region, Head and neck cancers (HNCs) correspond to a heterogeneous group of diseases, including *epidermoid carcinoma (squamous cell carcinomas that represent the 90 % of cancers in this anatomical segment)* of the pharynx, larynx, and oral cavity, as well as glandular tumors (salivary and thyroid glands). They represent a highly challenging pathology, considering the anatomical complexity of the cervico-facial region and the functional and aesthetic repercussions that both the disease and its treatment can produce (1). Likewise, our social interactions depend largely on structures located in this area, such as the larynx, the voice-producing organ, and the face, considered as a fundamental structure for the interaction, understanding and establishment of human relationships.

It is the sixth cancer in incidence worldwide and the eighth in mortality, with more than 630,000 new cases every year and a low long-term survival rate, around 50 % (2). More than 90 % of them are of squamous histology, having aggressive behaviors, even compromising organs and tissues in post-treatment stages (2,3). In relation to the rest of the histology, 2 % are sarcoma and 7 % are adenomas, melanoma and unspecified. In Spain, according to data from the *Spanish Society of Otolaryngology and Head and Neck Surgery (SEORL-CCC)*, every year, 10,000 new cases are detected, especially in people between 45 and 65 years (4).

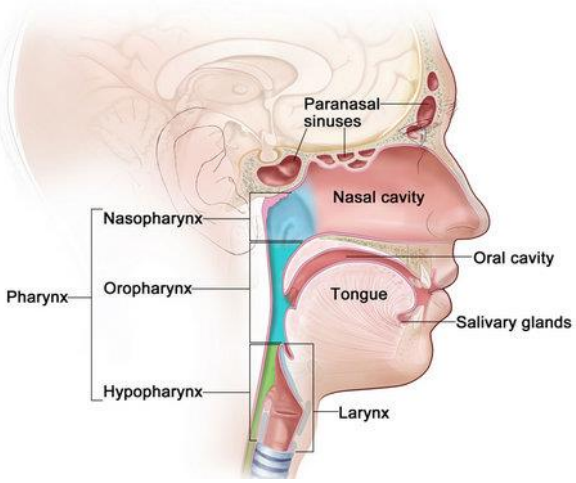

Image 1: The basic parts of Otorhinolaringologic anatomy.
Picture Source: *www.ncbi.nlm.nih.gov*.

Risk Factors:

The classic risk factors directly related to the development of HNCs are the consumption of tobacco and alcohol, although there are other situations related to its appearance. Concerning tobacco, numerous epidemiological studies have revealed the relationship between tobacco consumption in all its forms and the HNCs, as well as the reduction of risk when this habit is abandoned (5–7). The carcinogenic activity resides in the different particles contained in tobacco smoke that act as initiators, promoters or as carcinogens. The highest risk of HNCs in smoking patients is between three and 15 times compared to non-smokers and it is directly related to the dose and duration of consumption, as it has been seen more recently with the age of onset of consumption. Prolonged exposure to tobacco smoke in people who do not smoke is a recognized risk factor and is especially high in women and workers in a smoking environment. Regarding the alcohol, as well as in the case of tobacco, it is also considered an important promoter of carcinogenesis in HNC (8). In general, the consumption of tobacco and alcohol is the cause of almost 65 % of head and neck cancers. This risk seems to depend on the alcohol content of the drink. However, the greatest carcinogenic effect is due to the potentiation of the tobacco effect (9).

Another main risk factor for HNCs are certain infections such as Epstein-Barr virus (EBV) and human papillomavirus and subtype 16 (HPV-16) (10). The relationship of HPV-16 with HNCs has been especially evident in oropharyngeal neoplasms and is not related to tobacco consumption. A higher incidence of this type of tumor has been found in individuals with some sexual practices. Recent studies connect the presence of HPV in patients with oropharyngeal tumors with response and survival. Regarding EBV, the association with nasopharyngeal cancer has been revealed in multiple epidemiological studies (11,12).

Other less important factors are the diet, with an inverse relationship between the incidence of HNCs and the consumption of fruits, vegetables, fresh products and olive oil and the direct consumption of animal fat, smoked and salted fish, as well as fried foods (13). Although global exposure to occupational factors plays a limited role in the HNCs, in some specific cases it is a relevant aspect. Therefore, there is a clear increased risk of breast cancer in workers in the metallurgical, wood, textile and leather industries.

Finally, in terms of genetic susceptibility, studies in population groups have shown a three to eight times greater risk of suffering a HNCs in people with a history in first-degree relatives, which implies genetic susceptibility in its appearance (14).

Diagnosis:

These tumors manifest clinically as palpable masses or by the production of persistent symptoms in the upper aero-digestive tract. Faced with symptomatology and a suspicious medical history, samples are usually taken by biopsies, smears, exfoliated samples or saliva to study tumor markers. Endoscopic studies are also usually done to complete the evaluation of the patient. In the same line imaging techniques such as nuclear magnetic resonance, computed tomography and positron emission tomography

studies using radioisotope markers have increased sensitivity in the detection of small primary tumors, colonizing the lymph nodes, which are not palpable or visible in routine clinical examination. Moreover, histopathology is essential to determine the definitive diagnosis(9).

Besides, to perform a correct treatment, we must first carry out an adequate staging of the tumor, which in turn will allow us to predict the prognosis of the disease. To determine the prognosis of the disease, we use a classification system developed by the Union for International Cancer Control and which is still in force today. This classification considers three important aspects in the progression of a neoplastic process, such aspects are the size of the tumor that is designated with the letter "T", the presence of lymph nodules affected by the loco-regional dissemination of tumor designated with the letter N and finally the presence of distant neoplastic cells, which is known as tumor metastasis and is designated with the letter M. In its set, it is known as the TNM classification system, which is the most used classification to sort HNCs and other tumors. Thus, tumors are classified from stage I to stage IV (15). The management of HNCs must be carried out by multidisciplinary teams, with surgery and radiotherapy the pillars of treatment.

Treatment

Currently, treatment for head and neck cancer can include surgery, radiation therapy, chemotherapy or a combination of treatments. But these types of treatments are usually quite aggressive, they can also cause side effects and generate sequelae that can end up altering both the functionality and the aesthetics of the face and the surrounding regions. The technique, it is too complex for the surgeon due to the difficult anatomical relationships of this region which makes surgeries hard to perform and the presence of a multidisciplinary group is needed. Often, surgery for HNCs the patient's ability to chew, swallow or talk. The patient may look different after surgery, and the face and neck may be swollen. The swelling usually goes away within a few weeks. However, if lymph nodes are removed, the flow of lymph in the area where they were removed may be slower and lymph could be collected in the tissues, causing additional swelling; this swelling may last for a long time. After a laryngectomy or other surgery in the neck, parts of the neck and throat may feel numb because nerves have been cut, sometimes alteration in voice emission can occur as a complication of surgery. Otherwise, patients who receive radiation to the head and neck may experience redness, irritation, and sores in the mouth; a dry mouth or thickened saliva; difficulty in swallowing; changes in taste; or nausea. Other problems that may occur during treatment are loss of taste, which may decrease appetite and affect nutrition, and earaches (caused by the hardening of ear wax). Patients may also notice some swelling or drooping of the skin under the chin and changes in the texture of the skin. The jaw may feel stiff, and patients may not be able to open their mouth as wide as before treatment (16).

The treatment of these tumors should balance the oncological effectiveness with the maximum preservation of function and physical appearance, achieving a quality of life acceptable to the patient. Because of the disadvantages of current treatment, there is an urgent need to develop different therapies that can improve treatment, making it

less aggressive and less deforming, guaranteeing better therapy and ultimately improving the patient's quality of life. In this work, we propose Nanomedicine as a novel tool for the treatment of this type of tumors since it offers multiple advantages both in its less aggressive application and in the development of more specific therapeutic routes (17).

Nanotechnology and Nanomedicine:

Nanomedicine is the application of nanotechnology to achieve innovation in healthcare. It uses the properties developed by a material at its nanometric scale (10^{-9} m) which offers differ in terms of physics, chemistry or biology from the same material at a bigger scale (18). Image 2 shows a comparison that reflects the different sizes and includes the size range of the materials in the nanometric range.

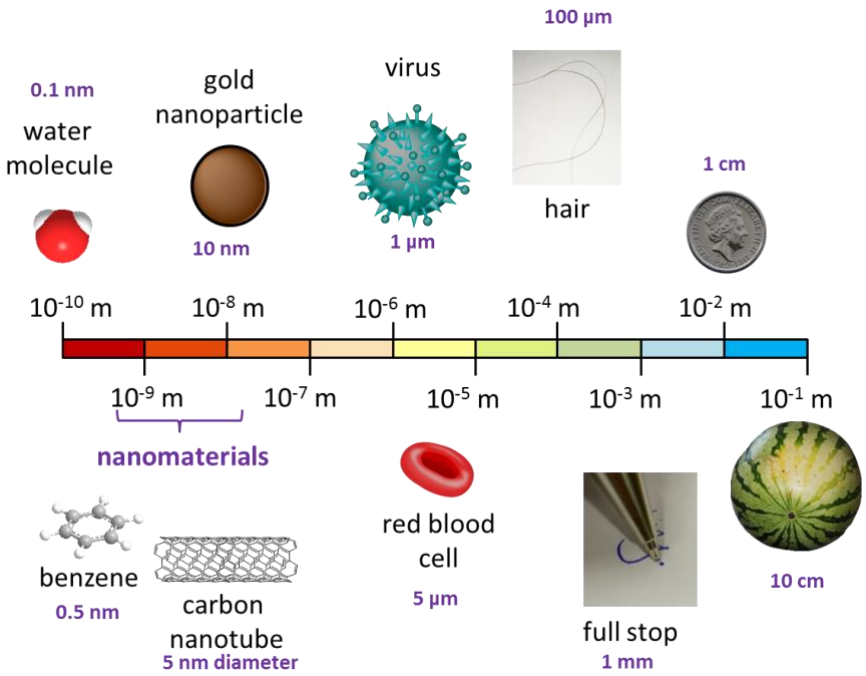

Image 2: Representative difference scale sizes in comparison to the range Nanometric.
Picture source: *https://chembam.com/definitions/nanotechnology/*

Furthermore, the nanometric scale is at the same time the range of size of many physiological mechanisms in the human body, allowing nanomaterials to traverse natural barriers to access new delivery sites and be in contact with DNA or proteins at different levels such as blood, organs, tissues or cells. At the nanometric scale, the surface-volume ratio is related to the properties of the surface of particles, changing the potential actions of a particle to ease the linking of other synthetic or biological materials. In this way, the coating of the particles and the functionalization of their surfaces (even at multiple levels) are extremely common to increase the biocompatibility of the particle and its circulation time in the blood, as well as to ensure a highly selective binding to the desired target (18).

Within Nanomedicine, we find different applications such as diagnosis, regeneration and its use as drug delivery systems. According to this last block, nano delivery systems are new but quickly developing science where materials in the nanometric range are employed to perform as tools of diagnostic or to deliver therapeutic agents to specifically target sites in a controlled way (19). Lately, there are many noteworthy implementations of the nanomedicine (chemotherapeutic agents, biological agents, immunotherapeutic agents etc.) in the treatment of several diseases. Drugs with very low solubility possess various biopharmaceutical delivery issues including limited bioaccessibility after intake through the mouth, less diffusion capacity into the outer membrane, require more quantity for intravenous intake and unwanted after-effects that appear in the traditional process of delivery. However, all these limitations could be overcome by the application of nanotechnology approaches in the drug delivery mechanism. Nanotechnology offers multiple benefits in treating acute and chronic human diseases by site-specific, and target-oriented delivery of precise medicines(20). The fact of encapsulating drugs in nanotransporters confers multiple advantages such as: increasing the solubility of drugs, the possibility of directing the drug and therefore, reducing the effective dose and reducing toxic effects with the consequent reduction of side effects. To target the drug to tumors, nanotechnology offers us two strategies: active and passive targeting.

Passive and active targeting

It has been known for quite some time that within the tumor architecture are established a series of different conditions those established in healthy tissues, such as inflammation (21), hypoxia (22) and the production of a multitude of cytokines and other vascular growth factors. All of them are involved in tumor response to satisfy their nutritional demands, thus generating a new formation of blood vessels and an increase in vascular permeability mediated by vasoactive substances released by diseased cells (23).

The enhanced permeability and retention effect (EPR) was discovered in 1986 by *Matsumura* and colleagues (24) and it refers the property which small sized nanoparticles and macromolecular drugs can accumulate more in tumor than in normal tissues. The EPR effect, as it can be seen in the image 3, is generally caused to the larger pore size of neo-vasculatures and poor lymphatic clearance of tumors, of this way these newly formed leaky vessels allow a selectively enhanced permeation of macromolecules larger than 40-50 kDa which showed more accumulation in tumor tissues than in healthy ones, and it is strongly influenced by the size of small molecules including nanoparticles (25). This selectivity is not valid to small molecule drugs which have short circulation time and quick washout from the tumour. Hence, the encapsulation of small molecule drugs in nanosized drug carriers improves their pharmacokinetics (prolonged systemic circulation), provides some tumour selectivity and decreases side effects (26). This type of tumour-targeting called *passive* is based on the characteristics of the carrier (size, circulation time and fast washout) and the biology of the tumor (vascularization, leakiness, etc.), but does not have a ligand for the specific binding to tissues or organs.

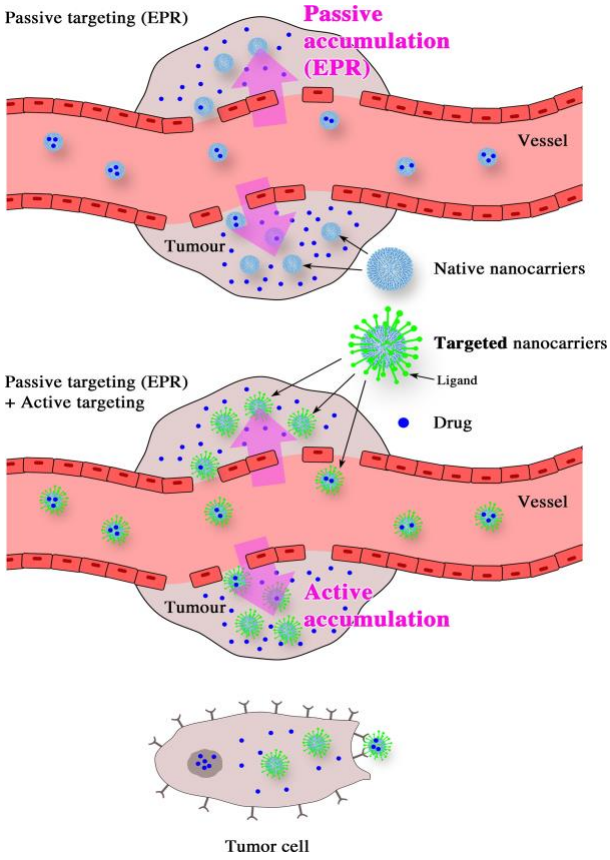

Image 3: Scheme illustrating the passive targeting (EPR) and the active targeting into a tumour. Picture source: https://onlinelibrary.wiley.com/doi/10.1111/jphp.13098

In other cases, it is necessary to further increase the affinity of our carriers towards a specific molecular target, this is required in cases where we want to decrease the toxicity generated by the drug or in those cases in which the internalization of the drug is difficult to carry out. To achieve this goal, the carriers are coated with specific ligands that will recognize specific molecules in the target cells, thus generating greater specificity (26). This is known as *active targeting* and it is essential for the delivery of drugs, genes and theranostics to the location of interest avoiding the normal tissues and thereby enhancing the therapeutic efficiency and limiting the side effects. Some examples of active targeting can be molecular ligands such as: peptides, proteins, vitamins, growth factors, etc. which, arranged on the surface of the particle, can interact with the surface of cell membranes and enter through mechanisms dependent on endocytosis (27). Of this way, active targeting can significantly increase the quantity of drug delivered to the target cell compared to free drug or passively targeted nanosystems. The first evidence of this phenomenon was proposed in 1980 with antibodies grafted in the surface of liposomes (28) and the other several types of ligands as peptides, nucleic acids, aptamers among others (29,30).

With the progression of nanomedicine and, due to the advances of drug discovery/design and drug delivery systems, numerous therapeutic procedures have been proposed and traditional clinical diagnostic methods have been studied, to increase the drug specificity and diagnostic accuracy (31). For instance, new routes of

drug administration are being explored such as oral, transdermal, ocular and transmucosal routes using dendrimers as delivery systems (19,31), and there is focus on ensuring their targeted action in specific regions, thus reducing their toxicity and increasing their bioavailability in the organism (32).

In the same line of research is our work, we intend to find a route of drug administration that is biocompatible with cellular models of squamous cell cancer that can later be extrapolated to humans, while trying to find a specific route of administration that guarantees a better arrival of the drug with fewer side effects and that is as specific as possible against the tumor we want to treat. The overexpression of cellular receptors of interest in cancer therapeutics is widely known and new molecular targets are sought every day to serve as a vehicle for drug entry. For a similar purpose, the Globotriaosilceramide (GB3) has been described in the scientific literature as present in HNCs (33), in malignant gliomas and meningiomas, more precisely Gb3 was predominantly found in the tumor vasculature (34,35) among other cancers such as Burkitt's lymphoma (36) and fibrosarcoma-associated antigen in rats (37). That is why in our work, focused on HNCs, we will use the GB3 receptor as a target molecule, explained in the next point 1.3, which is naturally present in the epithelial cells of the digestive tract and is particularly overexpressed in some digestive cancers (38,39). Based on this fact, it has been thought to use the Shiga toxin (Stx), which has a specific affinity for this receptor (specifically the B subunit), as a vehicle molecule for the specific administration of anti-tumor drugs in this type of cancer that overexpress the mentioned receptor.

Mesoporous Silica Particles:

There are different types of nanomaterials that have been used as targeted carriers. Among others, the most employed are liposomes, polymeric micelles, carbon nanotubes, dendrimers, inorganic particles and silica-based materials (image 4). Some of them as Mesoporous silica particles (MSPs) have attracted much attention due to their singular properties. They have a well-defined internal mesopore structure (from 2 to 10 nm of diameter) with a large pore volume (0.6-1 cm^3/g) and a high surface area (700-1,000 m^2/g). Their size, nano- (50 nm) to submicron-scale (500nm), as well as their shape and surface, can be custom-designed offering many different possibilities for the loading of anticancer drugs such as Docetaxel, Paclitaxel or Doxorubicin, among many others(40).

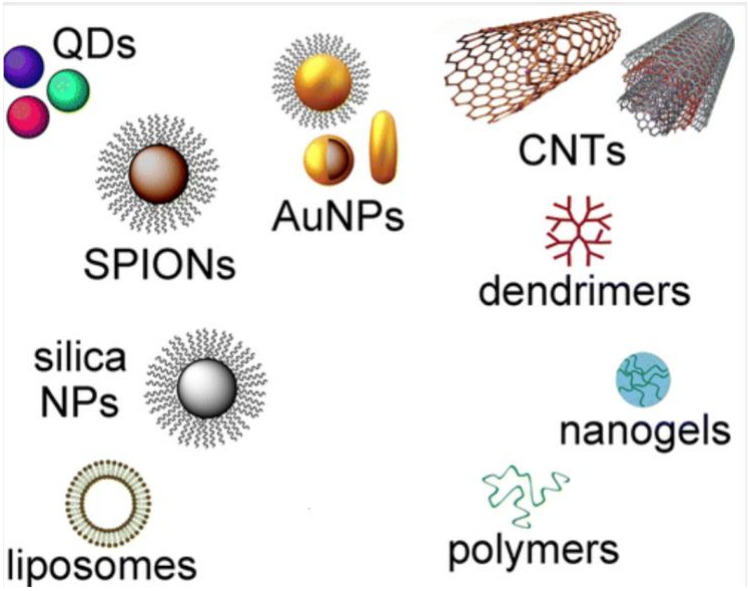

Image 4: Different types on nanomaterials in medicine.
Picture source: https://pubs.acs.org/doi/pdf/10.1021/ml3003742

Moreover, the cytotoxicity of these particles and cellular uptake have been demonstrated to be dependent on nanoparticle size and surface change. Indeed, 15 nm diameter particles have been reported to trigger more cytotoxicity than 100 nm diameter particles in endothelial cells. Some researchers have reported that there is an optimal size of silica particles to work with, and they found that this optimal size is 50 nm diameter (41).

Thus, their unique properties of tunable pore size, pore-volume, high loading capacity makes them widely exploited nanocarriers. Varying the molar composition of the reactants, type of reactants and the reaction conditions, MSPs with different particle size, shape and pore volume can be obtained. Tailoring the surface properties and pore size of MSPs helps enhance the loading and modify the drug release profile. The major research on MSPs is focused on the use of them in the treatment of cancer wherein a variety of ligands can be anchored onto the surface of MSPs due to the ease of functionalization. Moreover, these smart systems can be used to deliver drugs at the site of interest by various external and internal stimuli such as pH, temperature, light, chemicals, enzymes, ultrasound and so forth (42).

Different studies have demonstrated that silica nanoparticles are not toxic when administrated to different cell types to different dosages (43). Another characteristic of the MSPs that we should mention is their biocompatibility. Many studies have been done on the viability of particles and some have shown that MSPs can be degraded in water and phosphate-buffered saline (44). There are a series of parameters that can trigger the degradation of MSPs *in vitro* that include the morphology of the particle, the surface area and the functionalization surface, among others. For example, spherical particles are more degradable than rod-shaped particles (42). It should also be said that some of the characteristics of the particles such as the electrical charge they possess make them more easily eliminated by renal clearance or the faeces when they are

positively charged (45,46). Some lipid-coated particles make them more biocompatible by mimicking cell membranes (47) and other PEGylated particles have turned out to be more resistant to degradation because they escape recognition by the phagocytic mononuclear system (liver and spleen mainly), thus achieving a longer half-life in blood circulation (48).

Therapeutic targets: GB3 receptor:

GB3 Receptor and Cancer

The search for effective cancer therapies has been increasingly difficult due to the enormous general complexity intrinsic to tumors (49) and the great diversity of them both in cell types, in expression molecules and the development of a tumor microenvironment (50).

For this reason, new forms of treatment are investigated to be more specific, designed against determined cell types, which provide great tumor specificity, making new therapies act only on sick cells. Therefore, it is necessary to have an exhaustive knowledge of the tumor microenvironment (51) to be able to design the necessary tools that attack the tumor either by inhibition of components of the extracellular matrix (52), such as fibroblast growth factors among others (53), or inhibiting hypoxia generated by growing tumor cells that triggers a series of cellular responses to counteract oxygen deficiency, primarily coordinated by hypoxia-induced transcription factor 1 (HIF-1) (54). We can also design therapies that neutralize angiogenesis signals, such as vascular endothelial growth factor A (VEGFA) which induces the angiogenesis response after binding to the VEGF 2 receptor (VEGFR-2) located on the surface of endothelial cells present in neighbouring endothelial cells (55).

Gb3 is a glycosphingolipid from the group of globosides which is formed by the alpha linkage of galactose to lactosylceramide catalyzed by Lactosylceramide 4-alpha-galactosyltransferase (56). Glycosphingolipids are ubiquitous components of the cell membranes and they are almost exclusively located in the outer leaflet enabling them to play a role as specific mediators for cell adhesion and intercellular recognition (57). These cell membrane receptors have been implicated in oncogenic transformation processes due to changes in their composition and metabolism (57). In this work focused on HNCs, the Gb3 receptor has been proposed as a molecular target for treatment in cancer due to its overexpression in many tumors as we have mentioned previously.

Molecular ligands for Gb3

The natural ligands for Gb3 are Shiga toxins, which belong to a family of related protein toxins secreted by some types of bacteria. Shiga toxin is produced by *Shigella dysenteriae* (58), whereas the Shiga-like toxins, Stx1 and Stx2, with a few known isoforms, are secreted by specific strains of *Escherichia coli* named Shiga-toxin-producing *E. coli* (59). These toxins can produce different conditions in humans, from mild diarrhea to hemorrhagic colitis, and can progress to hemolytic uremic syndrome (HUS), accompanied by hemolytic anemia, thrombocytopenia, and severe acute kidney failure (60).

These toxins are composed of two main subunits as shown in image 5, an A subunit that binds non-covalently to a pentamer of five identical B subunits (AB5). The A subunit of the toxin damages the eukaryotic ribosome and inhibits protein synthesis in target cells. The function of pentamer B is to bind to the Gb3 cell surface receptor, which is found mainly in endothelial cells. The mature A subunit has a trypsin sensitive region that allows the subunit A to be cleaved asymmetrically into an A_1 subunit and A_2 peptide held together by a disulfide bridge. The enzymatic activity of the toxin resides within A_1 while the A_2 peptide tethers A_1 to the binding moiety, and further, threads through the B pentamer (61). Gb3 clusters within detergent-insoluble portions of membranes called "lipid rafts" which also contain cholesterol and the cholera toxin receptor monosialotetrahexosylganglioside or GM1 (62). It has been observed that the interaction of the Stx1 B subunit with HeLa cells causes a 2.5-fold increase in Gb3 present in the lipid raft domains, a result that suggests that cell binding by the B pentamer may promote stronger or additional toxin/cell interaction by recruiting more receptors to the rafts (61).

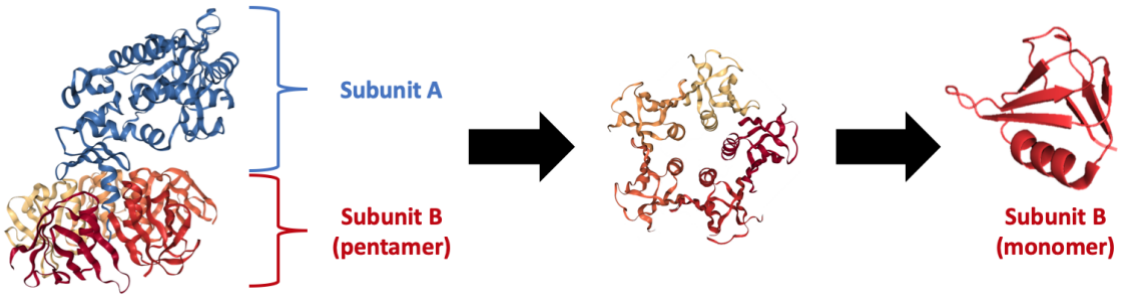

Image 5: A 3d model of Stx protein.

After binding to Gb3, the toxin/receptor complex enters early endosomes, then traffics to the Golgi, and finally the Endoplasmic Reticulum (ER) (63). The protease-sensitive site of the toxin A subunit is nicked either within the intestinal mucus or within the Golgi (64). However, the nicked toxin retains the AB5 structure because of a disulfide bond between the A_1 and A_2 chains. The disulfide bond is reduced once the toxin gets into the ER, and only the toxin A1 subunit enters the cytosol. An unfolded toxin A1 chain exits the ER, apparently by subverting the ER-associated protein degradation (ERAD) pathway, to reach the target ribosomes, then removes an adenine from the alpha-sarcin loop in the 28S ribosomal subunit. The injured ribosome no longer associates with elongation factor 1, and protein synthesis is halted (61).

Bearing all this in mind, the main aim of this project is to target-deliver Paclitaxel to head and neck cancer cells. For this purpose, we have encapsulated this drug together with a fluorescent dye within 500 nm diameter silica particles. These drug nano-carriers will be next coated with recombinant Shiga toxin, and administered in vitro to head and neck cancer cells (Detroit 562, a Human caucasian pharynx carcinoma cell line derived from pleural fluid of an adult female with primary carcinoma of the pharynx).

GOALS AND OBJECTIVES

Overall objective

The general objective of this Final Degree Project is to develop a targeted anti-tumor drug delivery system to be applied as a therapeutic method topically in head and neck cancer.

Specific objectives

The specific objectives that have been proposed to achieve the final objective of this final degree project are the following:

1. Encapsulation of an antitumor drug, called Paclitaxel, in silica nanoparticles.
2. Design, synthesis and modification of biocompatible Silica nanoparticles, functionalized with a protein coating.
3. Production and purification of a ligand-protein based on the B domain of the Shiga toxin, to biofunctionalize and target Nanoparticles to cancer receptors.
4. Study of the selective interaction and entry mechanism of functionalized nanomaterials with the ligand-protein in Head and Neck Cancer tumor cells.
5. Evaluation of the release and therapeutic effect induced by fluorescent Paclitaxel as an antitumor drug from Nanoparticles internalized in HNC tumor cells.

MATERIALS AND METHODS

Nanomaterials

Synthesis of the mesoporous silica particles (MSP)

The nanoparticles with which we are going to carry out this work have been designed and synthesized at the Department of Physical Chemistry of the University of Vigo by Dr. Miguel Á. Correa Duarte, based on Stober's modified method described in the literature (65). For this purpose, 0.8575 gr of K_2HPO_4 were first weighed and placed in a three-necked flask (250 mL). Then, 0.145 gr NaOH were weighed and dissolved in 10 mL of H_2O. After NaOH was added to the flask, H_2O was added to a final volume of 100 mL. 15 mL of glycerol were also added and the system was heated under reflux to 95 °C, under magnetic stirring (with a stir bar). When its temperature was stabilized at 95 °C, 0.4556 gr of CTAB were dissolved in 10 mL H_2O (apply heat to achieve its dissolution) and introduced into the flask. 250 µL of TEOS were added every 30 minutes through the septum with a syringe (12 times, for 6 hours in total). After the last addition, the reaction was kept for an additional 2 hours under stirring. Once the mixture was cooled (8 hours), the sample was washed 5 times. The first wash in a mixture with equal proportions of H_2O and ethanol (1:1) at 3300 g, 10 minutes, and the following in ethanol (3300 g, 10 minutes). Once the particles were synthesized, the surfactant (CTAB) was removed by thermal calcination at 600 º C for 6 h.

Encapsulation of Paclitaxel inside MSPs

The drug that we use in this study is Paclitaxel. Moreover, to facilitate the visualization by confocal microscopy of the drug, we use the Taxol Janelia Fluor, paclitaxel that has a fluorescent dye attached. Taxol Janelia Fluor® 646 is dissolved in Dimetylsulfoxide (DMSO) at 10 mg/mL: from there, 20 µL have been taken (200 µg of drug) and have been added 30 µL more of DMSO and 950 µL of water: so that the concentration of the drug is 200 µg/mL and the concentration of DMSO is 5 %. To perform this experiment 500 µg of SiO_2 particles are added to the previous solution. This mixture is left at room temperature for 3 hours with constant stirring. After 3 hours of incubation at room temperature, the excess of Taxol was washed by centrifugation-resuspension cycles in 5 % of DMSO at 7000 rpm for 10 minutes.

Recombinant Proteins

Recombinant Shiga toxin protein is a protein encoded by a gene produced synthetically and cloned in a bacterial expression plasmid. The synthesis of the protein is carried out by *Escherichia coli* (*E. coli*) bacteria that are widely used in biotechnology for recombinant protein production for diagnostic, therapeutics or vaccines, by relatively cheap procedures, since it has been very well characterized from the point of view genetic and physiological. Among the advantages that this microorganism offers as host are: i) higher specific growth rate than yeast and mammalian cells; ii) easy genetic manipulation, does not have costly requirements associated with culture media or

equipment, unlike cells from higher organisms; iii) existence of a wide variety of stable expression vectors, iv) and being a microorganism approved by regulatory entities for use as a host in the production of biopharmaceuticals (66).

In addition to the aforementioned, in this work we produce two types of proteins: on the one hand, we produce the ligand-protein which in this case is the Shiga toxin and, on the other hand, we produce the green fluorescent protein (GFP) -following the same procedures-, which we used to label the particles fluorescencently.

6xHis:GFP build design

Some organisms have evolved fluorescent molecules and other cell products (perhaps used to attract prey or defense against danger) that have been harnessed for research purposes. The jellyfish *Aequorea victoria* makes a protein called aequorin, which releases blue light after binding calcium. This blue light is then absorbed by another protein these organisms make, a green fluorescent protein (GFP) a 27 kDa β barrel-shaped protein, which in turn gives off a green light (67). Three scientists (*Shimomura, Chalfie* and *Tsien)* received the Nobel Prize in Chemistry in 2008 for isolating GFP from jellyfish, expressing it in other organisms, and mutating it to create fluorescent proteins in a variety of colors that can be expressed in cells as experimental markers(68). We worked with one of these versions of GFP fused to a sequence of 6 histidine residues at its N-terminus, a construction hereafter called 6xHis:GFP. With this construction, as will be seen in the following sections, the study of the utility of the histidine sequence as a structure for binding to the surface of SiO_2 particles was carried out, as well as evaluations of the stability of the binding against different terms.

The DNA sequence of this recombinant protein, collected in GenBank reference AAO20041.1 (NCBI), is as follows:

ATGGTGAGCAAGGGCGAGGAGCTGTTCACCGGGGTGGTGCCCATC
CTGGTCGAGCTGGACGGCGACGTAAACGGCCACAAGTTCAGCGTG
TCCGGCGAGGGCGAGGGCGATGCCACCTACGGCAAGCTGACCCTG
AAGTTCATCTGCACCACCGGCAAGCTGCCCGTGCCCTGGCCCACC
CTCGTGACCACCCTGACCTACGGCGTGCAGTGCTTCAGCCGCTACC
CCGACCACATGAAGCAGCACGACTTCTTCAAGTCCGCCATGCCCG
AAGGCTACGTCCAGGAGCGCACCATCTTCTTCAAGGACGACGGCA
ACTACAAGACCCGCGCCGAGGTGAAGTTCGAGGGCGACACCCTGG
TGAACCGCATCGAGCTGAAGGGCATCGACTTCAAGGAGGACGGC
AACATCCTGGGGCACAAGCTGGAGTACAACTACAACAGCCACAAC
GTCTATATCATGGCCGACAAGCAGAAGAACGGCATCAAGGTGAAC
TTCAAGATCCGCCACAACATCGAGGACGGCAGCGTGCAGCTCGCC
GACCACTACCAGCAGAACACCCCCATCGGCGACGGCCCCGTGCTG
CTGCCCGACAACCACTACCTGAGCACCCAGTCCGCCCTGAGCAAA
GACCCCAACGAGAAGCGCGATCACATGGTCCTGCTGGAGTTCGTG
ACCGCCGCCGGGATCACTCTCGGCATGGACGAGCTGTACAAGTAA

For our study, a fusion protein with 6 histidine residues was generated at the amino terminus of the GFP. The sequence of the complete protein is shown below, with the

histidine residues highlighted in blue and the GFP residues in green. This design was carried out by Drs. Esperanza Padín González and Mónica López Fanarraga:

MGSS**HHHHHH**SSGLVPRGSHMGTLELKLRKILQSTVPRARDPPVATM**VSKGEELFTGVVPILVEL DGDVNGHKFSVSGEGEGDATYGKLTLKFICTTGKLPVPWPTLVTTLTYGVQCFSRYPDHMKQH DFFKSAMPEGYVQERTIFFKDDGNYKTRAEVKFEGDTLVNRIELKGIDFKEDGNILGHKLEYNYN SHNVYIMADKQKNGIKVNFKIRHNIEDGSVQLADHYQQNTPIGDGPVLLPDNHYLSTQSALSK DPNEKRDHMVLLEFVTAAGITLGMDELYK**

The indicated genetic sequence was synthesized and cloned by the General Biosystems company (Morrisville, USA). The genetic construction resulted was sequenced for testing.

The genetic sequence is cloned into vector pET-15b (Novagen). In this vector, the cloned genes are under the control of bacteriophage T7 RNA polymerase, a highly specific polymerase by the action of its lac promoter, so that transcription of the genes of interest will only take place after the addition of the appropriate inductor. In the case of the lac promoter, it can be induced by isopropyl-β-D-1-thiogalactopyranoside (IPTG), a non-hydrolysable analogue of allolactose. In the absence of an inducer, thanks to the presence of the *lacI* sequence that encodes the LacI repressor protein, it prevents RNA polymerase from transcribing genes, so that the system remains inactive for the energy saving of the bacteria. The pET-15b vector also presents an ampicillin resistance gene, allowing a subsequent selection of the bacteria that have been transformed with the plasmid of interest.

With this sequence-containing plasmid, One Shot™ BL21(DE3)pLysS E. coli (Thermo Fisher) chemically competent bacteria were transformed. The plasmid pLysS is characterized by the production of T7 lysozyme to reduce the basal expression of the gene of interest and confers resistance to the chloramphenicol antibiotic. Following the transformation protocol provided by the cited company, a 50 µl vial of competent bacteria was thawed on ice, to which 1 µl of 6xHis:GFP DNA (10 ng) was added, and after mixing gently, it was incubated in ice for 30 min. It was then heated in a 42 °C bath for 30 seconds, then quickly put back on ice. 250 µl of preheated SOC (Super Optimal Broth) medium was added to the tube and allowed to grow at 37 °C with stirring at about 225 rpm for 1 hour. Two different volumes of the culture (20 µl and 200 µl) were then seeded on two plates with LB agar (Labkem) with ampicillin (100 µg/ml; Scharlau) and chloramphenicol (34 µg/ml; Fisher Scientific), and They were left to incubate at 37 °C overnight for the growth of bacterial colonies.

STxB:6His build design

Shiga toxin is one of the most potent bacterial toxins known. Stx is found in *Shigella dysenteriae* and in some serogroups of *Escherichia coli* (called Stx1 in *E. coli*). *S. dysenteriae* and the Stx were identified in the 19th century by Drs. Neisser, Shiga and Conradi. Approximately 80 years later the same toxin (now called Stx1 to distinguish it from the toxin produced by *S. dysenteriae*) was found in a group of *E. coli* isolates. These bacteria cause bloody diarrhea and some serious sequelae, the hemolytic uremic syndrome (HUS), a condition characterized by thrombocytopenia, hemolytic anemia,

and kidney failure. As we mentioned previously, the Stxs consist of two major subunits, an A subunit that joins noncovalently to a pentamer of five identical B subunits (each subunit = 69 aa). The A subunit of the toxin injures the eukaryotic ribosome, and halts protein synthesis in target cells. The function of the B pentamer is to bind to the cellular receptor, globotriaosylceramide, Gb3, found primarily on endothelial cells of the intestine, kidney, and the brain (69).

To produce a recombinant protein consisting of the B subunit of the Shiga toxin with a sequence of 6 histidines, a construction called STxB: 6xHis, a DNA construct was designed starting from the sequence of the B subunit of the Shiga toxin collected in GenBank reference NC_002695.1 (NCBI). This design was carried out by Drs. Elena Navarro Palomares and Mónica López Fanarraga. Finally, to this sequence was added at its 3' end another coding agent for six histidine residues, resulting in the following genetic construction:

ATGAAGAAGATGTTTATGGCGGTTTTATTTGCATTAGCTTCTGTTAATGCAATGGCGGCGGAT
TGTGCTAAAGGTAAAATTGAGTTTTCCAAGTATAATGAGGATGACACATTTACAGTGAAGGTT
GACGGGAAAGAATACTGGACCAGTCGCTGGAATCTGCAACCGTTACTGCAAAGTGCTCAGTT
GACAGGAATGACTGTCACAATCAAATCCAGTACCTGTGAATCAGGCTCCGGATTTGCTGAAGT
GCAGTTTAATAATGACCATC ATCACCATCACCATTGA

The amino acid sequence resulting from DNA transcription and translation would be as follows:

MKKMFMAVLFALASVNAMAADCAKGKIEFSKYNEDDTFTVKVDGKEYWTSRWNLQPLLQSAQL
TGMTVTIKSSTCESGSGFAEVQFNND**HHHHHH**

This construct was synthesized and cloned into vector pET-15b (Novagen) by General Biosystems. As in the case of the 6xHis:GFP, since it is the same vector, the expression of STxB:6xHis will occur after induction by IPTG, and the selection of transformed bacteria can be performed by adding ampicillin thanks to the corresponding resistance gene. The lyophilised provided by General Biosystems, 5 µg, was reconstituted in 50 µl of deionized distilled H2O to proceed to its transformation in the chemically competent One Shot™ BL21 (DE3) pLysS E. coli cells, following the same protocol described in the previous section. for 6xHis:GFP.

Overexpression of 6xHis:GFP and STxB:6xHis

To carry out the overexpression of the recombinant proteins, a colony isolated from the plates was inoculated with the BL21(DE3)plySs bacteria transformed with the corresponding plasmids, either to the 6xHis:GFP or STxB:6xHis construct, in 20 ml. LB nutrient culture medium (Labkem) was supplemented with ampicillin (100 µg/ml) and chloramphenicol (34 µg/ml). After leaving the pre-inoculum growing overnight, a 1:100 dilution of the pre-inoculum was performed to a larger volume of LB with ampicillin (100 µg/ml) for the subsequent induction of expression of the protein of interest. Once this dilution was made, the culture could grow at 37 °C until its optical density at 600 nm (OD_{600}) reached a value between 0.5-0.6, indicating that the bacteria are in their exponential growth phase and it is, therefore, the time-optimal for inducing protein

expression. For induction, in the case of 6xHis:GFP, IPTG (PanReac AppliChem) at a concentration of 0.7 mM was added to the bacterial culture and incubated at 37 °C for 4 h. For STxB:6xHis, IPTG was added at a concentration of 0.1 mM and incubated 15 h at room temperature. After the corresponding induction time, the bacterial culture was centrifuged at 4200 rpm for 30 min, the supernatant was discarded and the bacterial pellets were stored at -80 °C until use, or on ice if lysis was carried out immediately afterwards.

Bacterial lysis and protein extraction

To lyse the bacteria and obtain the soluble fraction of proteins, which will include the overexpressed 6xHis:GFP or STxB:6xHis protein, enzymatic digestion of the bacterial wall was carried out with lysozyme, followed by mechanical lysis by ultrasound to complement the breakdown. Thus, the bacterial pellets were resuspended in LEW lysis buffer (lysis buffer-equilibrated-wash) (50mM NaH_2PO_4, 300mM NaCl, pH 8) supplemented with 1 mg/ml lysozyme (PanReac AppliChem, 22500 U/mg) and protease inhibitor [1 tablet per 10 ml of buffer; Pierce Protease Inhibitor (Mini) Tablets (EDTA-free), Thermo Fisher Scientific] to prevent the degradation of the protein of interest by action of endogenous proteases of bacteria. Approximately, for the bacterial pellets corresponding to 250 ml of culture, 3 ml of supplemented LEW buffer were used. It was incubated with this buffer 30 min in the cold so that the lysozyme would work and then it was sonicated with a tip at 65 % of amplitude with sonication cycles of 15 seconds with 15 seconds of rest between cycles, up to a total of 5 min. Subsequently, it was centrifuged at 10,000 rpm for 30 min at 4 °C, and the supernatant was separated and filtered through a 0.45 µm pore size membrane to eliminate possible bacteria or aggregates that were present. In this supernatant is the total fraction of soluble proteins of the bacteria, among which is the overexpressed protein of interest to be purified in a subsequent step.

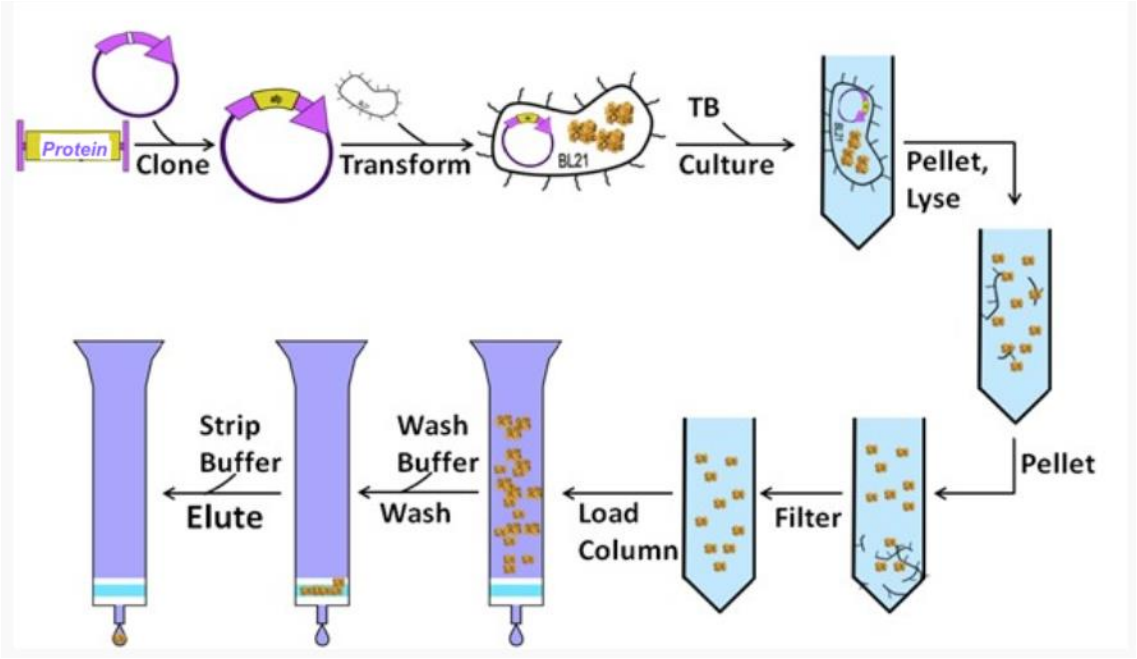

Image 6: General scheme of bacterial lysis and extraction and purification protein. Picture source: Univeristy of Washington (http://2009.igem.org/files/poster/Washington.pdf)

Purification of the recombinant proteins

For purification of 6xHis:GFP and STxB:6xHis, Nickel Protino Ni-TED 1000 columns (Machery-Nagel) were used. This purification is based on immobilized metal ion affinity chromatography (IMAC); the histidine residues of the protein bind to the Ni^{2+} ions of the column resin and then, thanks to a buffer with imidazole, this coordinates with the Ni^{2+} ions and displaces the bound protein.

Following the protocol indicated by the manufacturer, the column was first equilibrated with 2 ml of LEW 1X buffer (50 mM NaH_2PO_4, 300 mM NaCl, pH 8), and then the filtered bacterial lysis supernatant was added, at which time it remains the protein with the histidines bound to the column resin. After washing with 4 ml of LEW buffer to remove excess proteins that had not bound to the column, the bound protein was finally eluted by adding 4.5 ml of imidazole elution buffer (50 mM NaH_2PO_4, 300 mM NaCl, 250 mM imidazole, pH 8).

To remove imidazole from the solution so that it would not interfere with the subsequent functionalization of the NMs, a PD-10 desalination column with Sephadex® G-25 resin (GE Healthcare Life Sciences™) was used to transfer the protein to PBS 1X. For this, following the protocol, the column was equilibrated with about 24 ml of filtered 1X PBS. Then 2.5 ml of the purified protein was loaded and finally eluted in 3.5 ml of 1X PBS. To preserve protein in the short-medium term at 4 °C, sodium azide 0.1 % (w/v) was added.

SDS-PAGE electrophoresis

Discontinuous SDS polyacrylamide gel electrophoresis (SDS-PAGE) is one of the most widely used methods for the analysis of protein mixtures based on their molecular weights. It is a type of denaturing electrophoresis in which protein samples are denatured by heat and by treatment with reducing agents such as 2-mercaptoethanol, which breaks the disulfide bridges of proteins, and sodium dodecyl sulfate (SDS), which helps to denature and also, it gives proteins a net negative charge. Thus, they all travel towards the anode, separating based solely on their molecular weight. The molecular weight of any protein can then be determined by comparing with a standard of proteins of known molecular weights that are also loaded onto the gel.

This technique was used to verify the different fractions of the overexpression process in bacteria, as well as the subsequent extraction and purification of the recombinant proteins. It was also used in subsequent NM functionalization studies to analyze the bound protein on the surface. In the case of bacterial cultures, 500 µl samples were taken before and after induction, centrifuged at 13000 rpm for 10 min and resuspending the pellet in 50 µl of 1X loading buffer (stock 4X: Tris-Cl 200 mM (pH 6.8), 8 % SDS, 40 % (v / v) glycerol, 400 mM 2-mercaptoethanol, 0.4 % (w / v) bromophenol blue). Samples were also taken from all the steps in the protein lysis and purification process to evaluate its efficiency and locate in which fractions the protein of interest appears; In this case, 37 µl of each fraction was taken to which 13 µl of 4X loading buffer was added. All samples were heated at 95 °C for 10 minutes for protein denaturation before gel loading.

4 to 12 % gradient polyacrylamide gels (Bio-Rad) and 12 % other times (TruPAGE Precast Gels, Sigma-Aldrich) were used. The gradient gel allows a better separation of low molecular weight proteins, such as STxB:6xHis (<11 kDa). Electrophoresis was carried out in Mini-PROTEAN Tetra cell (Bio-Rad) cuvettes at a constant voltage of 180 V until the migration front reached the line marked on the gel cassette. 5 of the Precision Plus Protein™ Dual Color Standards (Bio-Rad) molecular weight standard, containing a mixture of 10 recombinant proteins of known molecular weights between 10 and 250 kDa were loaded onto each gel.

The technique used to detect the separated proteins in the polyacrylamide gels was Coomassie blue staining, a dye with a high affinity for proteins and which allows staining them in a simple way in the presence of an acidic medium. For protein fixation and staining, the gel was dipped in 2.5 % (w/v) Coomassie Blue (Fisher Bioreagents), 10 % (v/v) acetic acid (99 %, Cofarcas), and 45 % (v/v) methanol (extra pure, Scharlau). After 1 h, the staining was removed and the gel was stained in a solution with 10 % (v/v) acetic acid and 40 % (v/v) methanol, renewing the solution several times until they were well contrasted protein bands. For preservation and documentation, the gels were kept in distilled water. The gels were documented in the Doc™ EZ System (Bio-Rad) automated imaging system equipped with a CCD camera, to be subsequently analyzed with the Image Lab (Bio-Rad) program.

Cell Culture Assays

Cell lines used and culture conditions

To carry out this project, we worked with a single cell line. This cell line is known as Detroit 562, which corresponds to human squamous cell carcinoma obtained from pharyngeal cancer. This cell line has been maintained according to the supplier's recommendations (European Cell Culture Collection), that is, they have been kept in an incubator at a temperature of 37°C, with CO_2 levels of 95 % and relative humidity of 95 %. The manipulation of these cell lines was carried out under sterile conditions in class II laminar flow cabinet.

Cell Line	Tissue of origen	Species	Cell Line Description	Culture médium	Identification of ATCC
DETROIT 562	Pharynx	Human	carcinoma of the pharynx	MEM 10% FBS	ATCC® CCL-138TM

RESULTS AND DISCUSSIONS

Characterization of Particles:

In this final degree project, it has been chosen to work with SiO_2 due to its characteristics of being biocompatible, stable, with controllable thickness and porosity, as well as for having optical transparency. Besides to its potential use in cancer nanomedicine as we mentioned previously (see block Mesoporous Silica Particles).

The morphological characteristics and the dimensions of the particles (size and morphology) were evaluated with transmission electron microscopy (TEM). As can be seen in image 7, our particles have a spherical morphology and an average size of 527 nm.

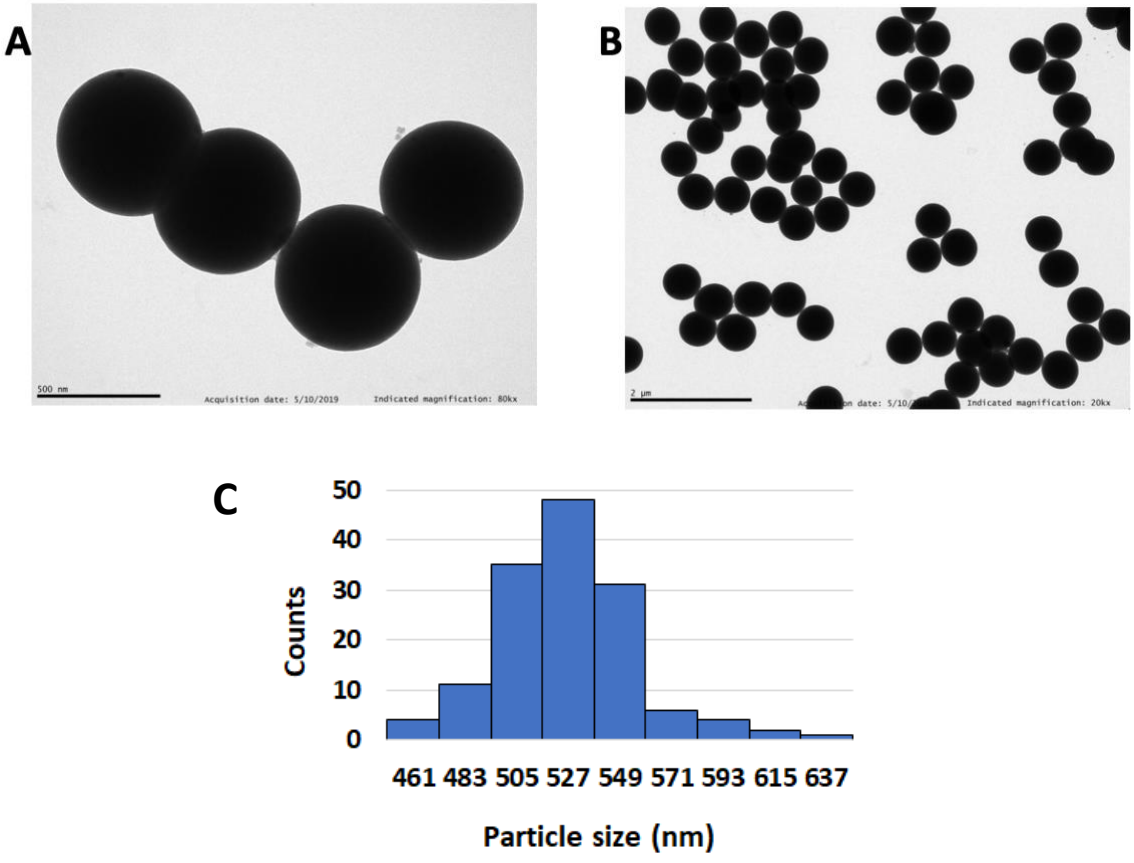

Image 7: TEM images and size distribution analysis of SiO_2 NPs. **(A**) Image of silica NPs with 80kx magnification. (**B**) Image of Silica NPs with 20kx magnification. (**C**) Size distribution of MSP with an average size of 527 nm.

Encapsulation of Paclitaxel

For the encapsulation of Taxol in the particles, 500 µg of SiO_2 were incubated with 200 µg of fluorescent Paclitaxel previously resuspended in DMSO and water. After the encapsulation process, the mix was centrifuged at 7000 rpm for 10 minutes as described previously in the Materials and methods section. Finally, two components were obtained in the Eppendorf: on the one hand, the pellet seen as a blue dot at the bottom of the Eppendorf tube (Image 8), and on the other hand, the supernatant that we will be used for its analysis of the encapsulation efficacy by visible ultraviolet spectroscopy.

Image 8: Silica nanoparticle pellet with Fluorescent Taxol.

Calibration curve

The calibration curve is a widely-used method in analytical chemistry to determine the concentration of a substance (analyte) in an unknown sample, especially in solutions. The method is based on the proportional relationship between the concentration and a certain analytical signal (property). The concentration-signal relationship is usually represented on a graph known as the calibration curve (70).

The analytical signal used must maintain a proportional relationship with the concentration. The most used signals are those whose relationship with concentration is linear, at least in the working range. For example, one of the most used properties is the absorbance (light absorption) that usually maintains a linear relationship with the concentration of solutes in solutions. Being a linear relationship, it can be represented by a line, hence this specific type of calibration curve is also known as a calibration line (71).

To prepare a calibration curve, several solutions are used with a known concentration of analyte that in our case is Taxol-5%-DMSO. These solutions are known as standard solutions. A battery of standards sufficient to cover a range including the expected concentration in the unknown samples was developed.

The concentrations used in the standards must also be within the valid range for the analytical technique to be used. That is, they must be above the minimum analyte concentration quantifiable by the technique used. This minimum is known as the quantifiable minimum limit. It must also be below the linearity limit. The linear relationship between concentration and signal is not usually maintained at high concentrations and the linearity limit marks the maximum concentration for which the calibration curve would be reliable.

As can be seen in this graph (Image 9), Taxol Janelia Fluor® 646 has a stable peak at a wavelength of 659.5 nm, that we are going to use to carry out the different measurements of our samples of known concentration and thus can carry out our standard line.

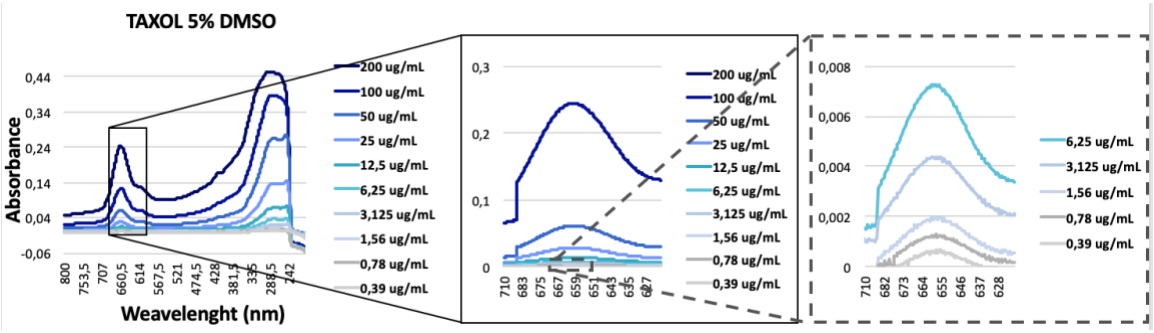

Image 9: Absorbation spectra of Taxol Janelia Fluor® 646 in 5 % DMSO at different concentration going from 200 µg/ml to 0.39 µg/ml.

The calibration curve is constructed by measuring the analytical signal in each of the previously elaborated standards. The measured Absorbance is assigned on the ordinate axis and the concentration of the standard on the abscissa axis. In this way, we can indicate points on the graph according to the coordinates (concentration (x), Absorbance (y)).

To these points, we can apply linear regression, generally by means of least squares adjustment, to obtain the line that relates them and their function $(y = 0{,}0006x + 0{,}0009)$ as seen in the imagen 10.

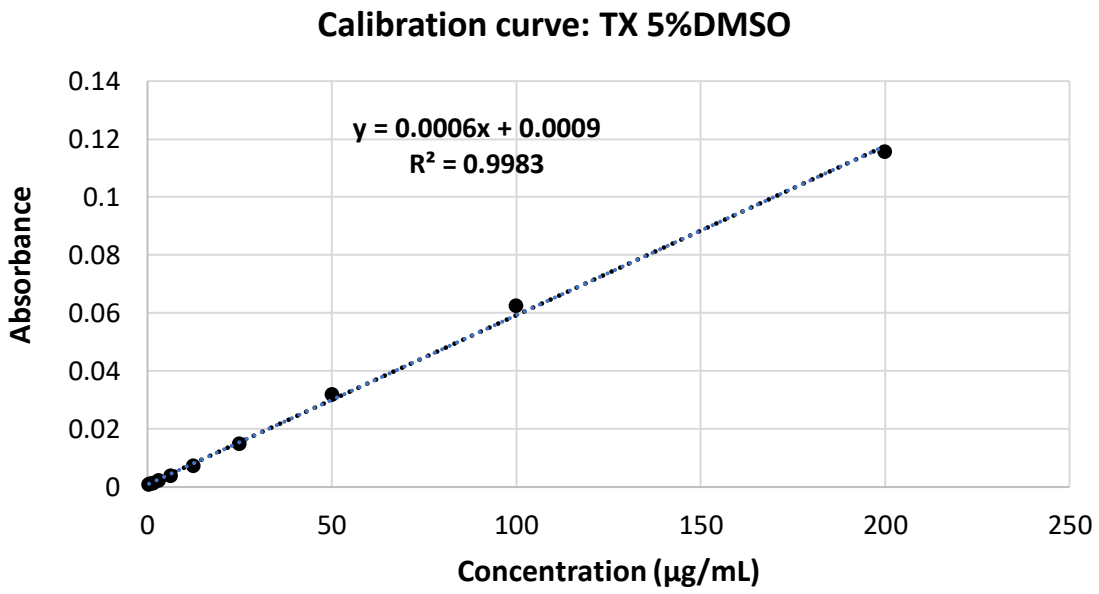

Image 10: Calibration curve that represents the relationship between Absorbance (ordinate axis) and Concentration of Tx-5%-DMSO (µg/ml).

Encapsulation efficacy of MSP

Once the calibration curve has been done, we have analyzed the supernatant of our encapsulated particles to see the total amount of drug that has not been encapsulated. The top of the image 11 shows an example of the supernatant spectra, and in the table of the bottom of the figure, we can see the absorbance of the washings of each experiment, and the concentration of the encapsulated drug, with a mean of an 86,6 % of encapsulation, which corresponds to 173.2 µg of the drug in 500 µg of particles. Thus, the encapsulation efficiency of these particles is very high, making this nanocarrier a potential strategy for the delivery of this drug.

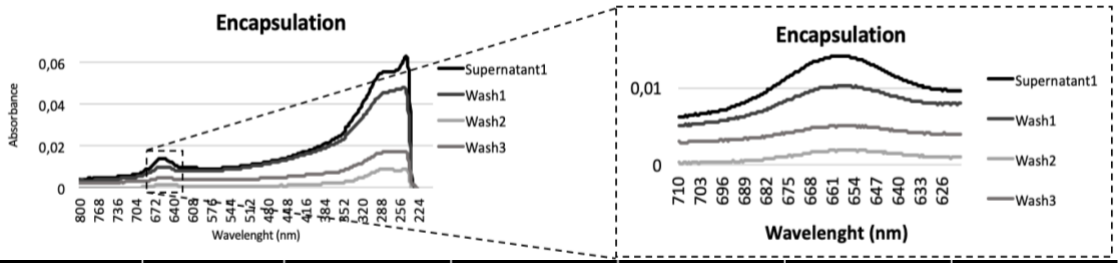

Washing	Absorbance (Exp1)	Concentration (µg)	Absorbance (Exp2)	Concentration (µg)	Absorbance (Exp3)	Concentration (µg)
Supernatant	0,0073	**10,69**	0,0164	**25,95**	0,00267113	**2,95**
1	0,0047	**6,38**	0,0004	**0,84**	0,0007631	**0,23**
2	0,0015	**1,08**	0,0015	**1,02**	0,00064901	**0,42**
3	0,0020	**1,83**	0,0027	**3,07**	0,00104439	**0,24**
4	0,0014	**0,82**	0,0037	**4,60**	0,00262012	**2,87**
5	0,0015	**0,96**	0,0032	**3,87**	0,0067197	**9,70**
TOTAL		**21,77**		**39,31**		**16,41**
Percentage		**89,1**		**80,3**		**91,8**
					Media	**86,8**

Image 11: Results of encapsulation of Taxol in Silica nanoparticles. (**Top**) Supernatant spectra and (**Bottom**) measurements of absorbance in different experiments with a mean of 86.6% of encapsulated drug.

Functionalization of MSPs with 6xHis:GFP and STxB:6xHis

Purification of 6xHis:GFP and STxB:6xHis

SDS-PAGE gel electrophoresis was performed to quantitatively and qualitatively verify the overexpression and purification of the bacterial proteins in the different fractions of the cultures of bacteria expressing the recombinant protein, as well as the subsequent extraction and purification of the recombinant protein (images 12 and 13). After induction of protein expression with IPTG for ca. 4 h at 37 °C for the GFP, and 12 h at room temperature for the STx (images 12, 13, lanes 2 and 3 respectively), the bands corresponding to 6xHis:GFP and STxB:6xHis displayed an approximate molecular weight of 27 and 10.7 kDa (green and red arrow, respectively). These bands do not appear in bacteria that had not been induced (lanes 1).

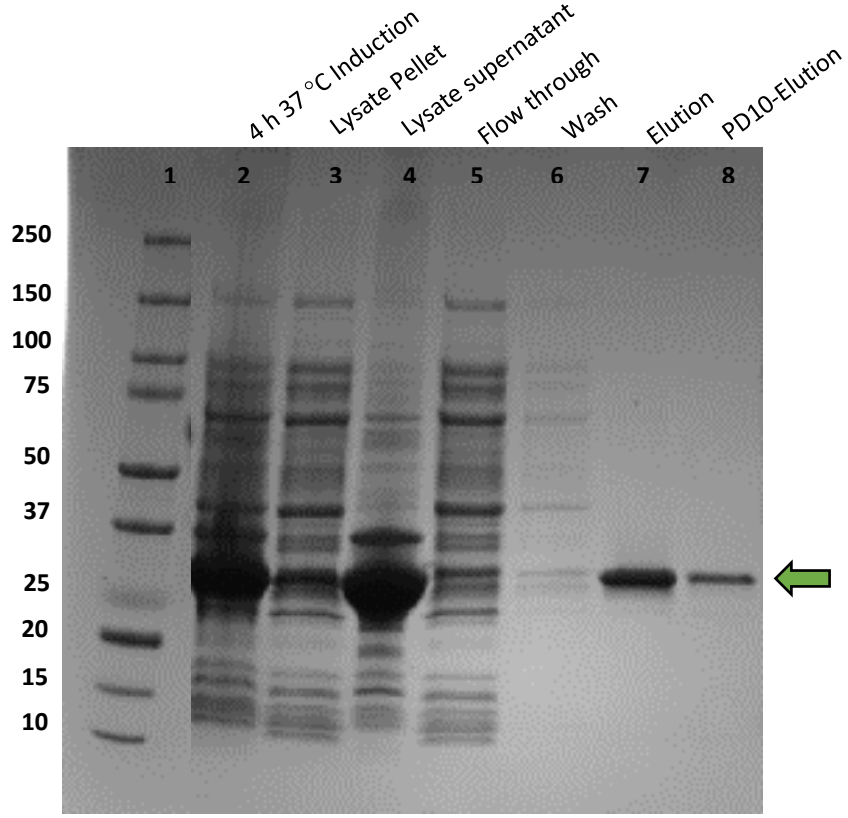

Image 12: SDS-PAGE analysis of the process of overexpression and purification of the 6xHis:GFP protein. On the top, the content loaded in each lane of the gel is listed. The green arrow points to the GFP.

After overexpression, a lysis of the bacterial wall, both enzymatic and physical, was performed to collect the protein of interest in the soluble fraction (image 12, 13; lanes 3 and 5) and thus proceed its purification. In lanes from 4 to 6 in 6xHis:GFP and from 6 to 8 in STx:&xHis, the different fractions of the nickel-protein chromatography column purification process appear, because the protein construct contains a sequence of 6 histidines with high affinity for nickel.

It is observed how in the protein fractions not bound to the column, the fraction called flow-through (lanes 5 or 6) and the column wash (lane6 or 7) all the bacterial proteins appear that are discarded as they have no affinity for the resin; A small amount of the protein of interest can also be seen by saturation of the column.

Finally, in the fraction collected after the addition of the buffer with imidazole (lane 8 in image 13), only the purified protein of interest appears. A sample after passing the purified protein through a PD-10 desalination column, used to remove the imidazole from the protein solution (lanes 8 and 10), was also loaded for checking.

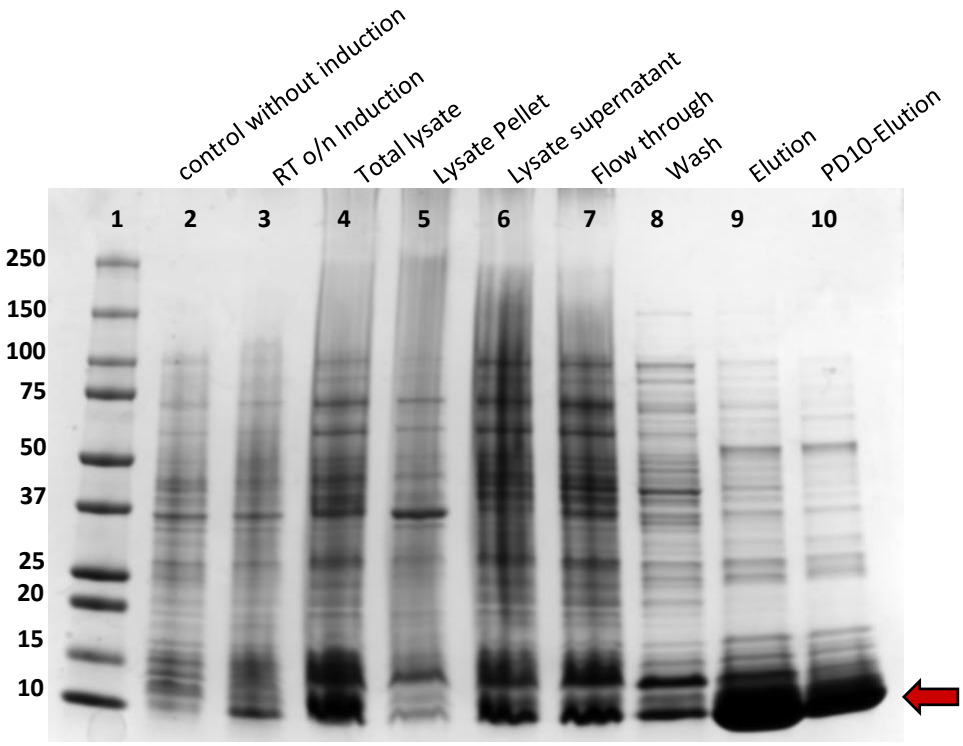

Image 13: SDS-PAGE analysis of the process of overexpression and purification of the STxB:6xHis protein. On the top, the content loaded in each lane of the gel is listed. The red arrow points to the STx.

Bioconjugation with 6xHis:GFP and STxB:6xHis

Taking advantage of the fact that the silica nanoparticles are negatively charged, a conjugation system with proteins has been developed through their binding to a positively charged amino acid sequence. For this experiment, we work with a tail made of 6 histidine residues. This work is based on the theses of Dr. Elena Navarro Palomares and Dr. Esperanza Padín Gonzalez, where they demonstrated that the presence of the 6xHis:GFP protein construct on the surface of the nanoparticles is mediated by the residues of the poly-histidine sequence.

As we have said throughout this work, one of the objectives is the treatment in a controlled and specific way to the HNCs, taking advantage of the overexpression of the Gb3 receptor in these cancers. To do this, we will use the bacterial Shiga toxin whose molecular target is the Gb3 receptor as a vehicle system for MSPs. In this way, we will create a chimera protein composed of the Shiga toxin interaction domain linked to a sequence of 6 histidines to later conjugate it with our MSPs. The ligand-protein used for this purpose was obtained by selecting the DNA sequence corresponding to one of the monomers that make up the Shiga toxin B subunit homopentamer (STxB) (See Material and Methods section), which has an affinity for the Gb3 receptor. In this way, the sequence corresponding to the catalytic subunit of the toxin, which is responsible for its harmful effect, was discarded. To this selected sequence, another codifier for 6 histidine

residues was added, thus obtaining a final sequence to get the fusion protein called STxB:6xHis (Image 14).

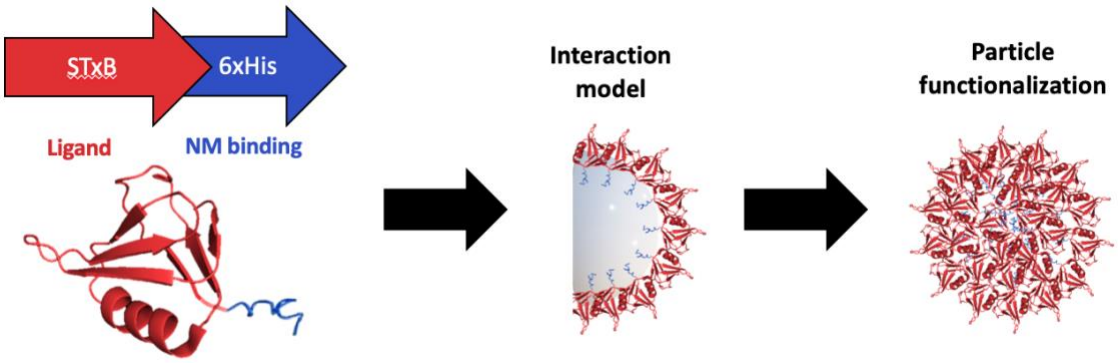

Image 14: Schematic representation of particle functionalization. (**A**) STxB:6xHis construction. (**B**) Particle functionalization.

Apart from the STxB:6xHis we conjugated our MSPs with GFP (10:1) in order to make the system visible by fluorescent confocal microscopy. To do this, the nanoparticles were bioconjugated by gentle sonication (3 cycles of 2 s) in a saline solution (PBS 1X) of the excess of both recombinant proteins. As mentioned before, the bioconjugated particle can be verified with the naked eye and with fluorescence microscopy due to the inherent fluorescence of GFP. Likewise, thanks to its fluorescence, the state of the folding of the protein can also be controlled to verify that it does not denature, that is, a decrease in fluorescence can be observed when its structure is significantly altered.

Ongoing Experiments:

To continue with the development of this final degree project, we had proposed carrying out some experiments that, due to unforeseen circumstances, could not carry out but may be resumed in the future. These experiments are the following:

Analysis of Gb3 receptor expression in Detroit 562 cells

As we have commented in this final degree project, we work with Gb3 receptor which is overexpressed in epithelial cells, being present in HNCs and gastrointestinal tumors (38). In this work, it has been decided to use head and neck cancer model cells named Detroit 562, an immortalized cell line derived from a human pharyngeal tumor which overexpresses the Gb3 receptor. Thus, we want to know the pattern of expression of Gb3 and the applicability of nanotherapies directed at said receptor. To characterize this receptor and visualize its location both at the cell membrane and intracellular level, a confocal fluorescence microscopy study will be performed of Detroit 562 cells stained with a specific anti-Gb3 antibody.

Administration of particles into Detroit 562 cells

This experiment aims to administer a known concentration of Taxol encapsulated in MSPs with our designed proteins coating in Detroit 562 cells and observe the expected phenotype. Paclitaxel prevents the formation of the mitotic spindle, binding to β-

tubulin, thereby promoting the formation of long polymers, even in the presence of GDP, which cannot be shortened. The paclitaxel-stabilized microtubule has 12 protofilaments (instead of the 13 normal protofilaments) and a diameter less than normal (22nm)(72). The stabilization of the microtubules causes the loss of function of the spindle, the consequent stop of the cell cycle in the metaphase/anaphase transition and, finally, cell death.

To perform this experiment we will use confocal fluorescent microscopy to observe the phenotype produced once taxol is released.

CONCLUSIONS

- Silica nanoparticles fulfil their function as nanocarriers for antitumoral drugs, entrapping 86.6% of Paclitaxel in their mesopores. The drug-filled particles can also be subsequently conjugated with recombinant proteins to guarantee the targeting to the Gb3 receptor.

- It has been possible to design and produce a targeting recombinant ligand-protein containing the sequence of the domain B of Shiga toxin fused to a positively charged sequence composed by 6 histidine residues, which serves for its stable and surface-oriented conjugation of nanomaterials with a negative surface charge.

REFERENCES

1. Barnadas Molins A, Arellano Tolivar A, Roca-Ribas Sardá F, Cuadras Collsamata P. Tumores de cabeza y cuello. Med - Programa Form Médica Contin Acreditado. 2001;8(56):3004–13.
2. Vigneswaran N, Williams MD. Epidemiologic trends in head and neck cancer and aids in diagnosis [Internet]. Vol. 26, Oral and Maxillofacial Surgery Clinics of North America. W.B. Saunders; 2014 [cited 2020 May 1]. p. 123–41. Available from: https://www.ncbi.nlm.nih.gov/pmc/articles/PMC4040236/
3. Leemans CR, Snijders PJF, Brakenhoff RH. The molecular landscape of head and neck cancer. Vol. 18, Nature Reviews Cancer. Nature Publishing Group; 2018. p. 269–82.
4. Sociedad Española de Otorrinolaringología y Cirugía de Cabeza y Cuello [Internet]. Madrid; Available from: https://seorl.net/cancer-cabeza-cuello-incidencia-espana/
5. Gandini S, Botteri E, Iodice S, Boniol M, Lowenfels AB, Maisonneuve P, et al. Tobacco smoking and cancer: A meta-analysis. Int J Cancer [Internet]. 2008 Jan 1 [cited 2020 May 1];122(1):155–64. Available from: http://doi.wiley.com/10.1002/ijc.23033
6. Kumar R, Rai AK, Das D, Das R, Suresh Kumar R, Sarma A, et al. Alcohol and tobacco increases risk of high risk HPV infection in head and neck cancer patients: Study from north-east region of India. PLoS One. 2015 Oct 16;10(10).
7. Jiang H, Livingston M, Room R, Gan Y, English D, Chenhall R. Can public health policies on alcohol and tobacco reduce a cancer epidemic? Australia's experience. BMC Med [Internet]. 2019 Nov 27 [cited 2020 May 1];17(1):213. Available from: https://bmcmedicine.biomedcentral.com/articles/10.1186/s12916-019-1453-z
8. Penfold CM, Thomas SJ, Waylen A, Ness AR. Change in alcohol and tobacco consumption after a diagnosis of head and neck cancer: Findings from Head and Neck 5000. Head Neck. 2018 Jul 1;40(7):1389–99.
9. GEORCC GMS y, SEOR G de E. Cancer Cabeza Y Cuello. Man Patol quirúrgica cabeza y cuello [Internet]. 2008;1–13. Available from: http://www.seor.es/wp-content/uploads/CANCER-DE-ORL-tratamientos-y-cuidados.pdf
10. Vietía D, Liuzzi J, Ávila M, De Guglielmo Z, Prado Y, Correnti M. Human papillomavirus detection in head and neck squamous cell carcinoma. Ecancermedicalscience. 2014 Oct 23;8.
11. Chien YC, Chen JY, Liu MY, Yang HI, Hsu MM, Chen CJ, et al. Serologic markers of epstein-barr virus infection and nasopharyngeal carcinoma in taiwanese men. N Engl J Med [Internet]. 2001 Dec 27 [cited 2020 May 1];345(26):1877–82. Available from: http://www.nejm.org/doi/abs/10.1056/NEJMoa011610
12. Siegel RL, Miller KD, Jemal A. Cancer statistics, 2017. CA Cancer J Clin [Internet]. 2017 Jan 1 [cited 2020 May 1];67(1):7–30. Available from: http://doi.wiley.com/10.3322/caac.21387
13. Sturgis EM, Wei Q, Spitz MR. Descriptive epidemiology and risk factors for head and neck cancer. Semin Oncol. 2004 Dec 1;31(6):726–33.
14. Dr. Ricardo Hitt Dra. Ana López Martín Dra. Anabel Ballesteros. Tumores cabeza

y cuello - O.R.L. - SEOM: Sociedad Española de Oncología Médica © 2019 [Internet]. 2017 [cited 2020 May 1]. Available from: https://seom.org/es/informacion-sobre-el-cancer/info-tipos-cancer/104033-tumores-cabeza-y-cuello-orl?showall=1
15. Cong L, Liu Q, Zhang R, Cui M, Zhang X, Gao X, et al. Tumor size classification of the 8th edition of TNM staging system is superior to that of the 7th edition in predicting the survival outcome of pancreatic cancer patients after radical resection and adjuvant chemotherapy. Sci Rep. 2018 Dec 1;8(1).
16. Clinical Trials Information for Patients and Caregivers - National Cancer Institute [Internet]. 2017 [cited 2020 May 1]. Available from: https://www.cancer.gov/about-cancer/treatment/clinical-trials
17. Chenthamara D, Subramaniam S, Ramakrishnan SG, Krishnaswamy S, Essa MM, Lin FH, et al. Therapeutic efficacy of nanoparticles and routes of administration. Vol. 23, Biomaterials Research. BioMed Central Ltd.; 2019.
18. What is nanomedicine? | ETPN [Internet]. [cited 2020 May 1]. Available from: https://etp-nanomedicine.eu/about-nanomedicine/what-is-nanomedicine/
19. Patra JK, Das G, Fraceto LF, Campos EVR, Rodriguez-Torres MDP, Acosta-Torres LS, et al. Nano based drug delivery systems: Recent developments and future prospects 10 Technology 1007 Nanotechnology 03 Chemical Sciences 0306 Physical Chemistry (incl. Structural) 03 Chemical Sciences 0303 Macromolecular and Materials Chemistry 11 Medical and He. Vol. 16, Journal of Nanobiotechnology. BioMed Central Ltd.; 2018. p. 1–33.
20. De Jong WH, Borm PJA. Drug delivery and nanoparticles: Applications and hazards. Vol. 3, International Journal of Nanomedicine. Dove Press; 2008. p. 133–49.
21. Torchilin V. Tumor delivery of macromolecular drugs based on the EPR effect. Vol. 63, Advanced Drug Delivery Reviews. 2011. p. 131–5.
22. D'Ignazio L, Batie M, Rocha S. Hypoxia and inflammation in cancer, focus on HIF and NF-κB. Vol. 5, Biomedicines. MDPI AG; 2017.
23. Fang J, Nakamura H, Maeda H. The EPR effect: Unique features of tumor blood vessels for drug delivery, factors involved, and limitations and augmentation of the effect. Vol. 63, Advanced Drug Delivery Reviews. Elsevier; 2011. p. 136–51.
24. Matsumura Y, Maeda H. A New Concept for Macromolecular Therapeutics in Cancer Chemotherapy: Mechanism of Tumoritropic Accumulation of Proteins and the Antitumor Agent Smancs. Cancer Res. 1986 Dec 1;46(8):6387–92.
25. Maeda H. The enhanced permeability and retention (EPR) effect in tumor vasculature: The key role of tumor-selective macromolecular drug targeting. Adv Enzyme Regul. 2001;41(1):189–207.
26. Attia MF, Anton N, Wallyn J, Omran Z, Vandamme TF. An overview of active and passive targeting strategies to improve the nanocarriers efficiency to tumour sites [Internet]. Vol. 71, Journal of Pharmacy and Pharmacology. Blackwell Publishing Ltd; 2019 [cited 2020 May 2]. p. 1185–98. Available from: https://onlinelibrary.wiley.com/doi/abs/10.1111/jphp.13098
27. González-Domínguez E, Iturrioz-Rodríguez N, Padín-González E, Villegas J, García-Hevia L, Pérez-Lorenzo M, et al. Carbon nanotubes gathered onto silica particles lose their biomimetic properties with the cytoskeleton becoming biocompatible. Int J Nanomedicine. 2017 Aug 29;12:6317–28.

28. Leserman LD, Barbet J, Kourilsky F, Weinstein JN. Targeting to cells of fluorescent liposomes covalently coupled with monoclonal antibody or protein A. Nature. 1980;288(5791):602–4.
29. Kamaly N, Xiao Z, Valencia PM, Radovic-Moreno AF, Farokhzad OC. Targeted polymeric therapeutic nanoparticles: Design, development and clinical translation. Vol. 41, Chemical Society Reviews. NIH Public Access; 2012. p. 2971–3010.
30. Wang X, Li S, Shi Y, Chuan X, Li J, Zhong T, et al. The development of site-specific drug delivery nanocarriers based on receptor mediation. J Control Release. 2014 Nov 10;193:139–53.
31. Mignani S, El Kazzouli S, Bousmina M, Majoral JP. Expand classical drug administration ways by emerging routes using dendrimer drug delivery systems: A concise overview. Vol. 65, Advanced Drug Delivery Reviews. 2013. p. 1316–30.
32. Lam PL, Wong WY, Bian Z, Chui CH, Gambari R. Recent advances in green nanoparticulate systems for drug delivery: Efficient delivery and safety concern. Vol. 12, Nanomedicine. Future Medicine Ltd.; 2017. p. 357–85.
33. Bolot G, David MJ, Taki T, Handa S, Kasama T, Richard M, et al. Analysis of glycosphingolipids of human head and neck carcinomas with comparison to normal tissue. Biochem Mol Biol Int. 1998;46(1):125–35.
34. Salhia B, Rutka JT, Lingwood C, Nutikka A, Van Furth WR. The treatment of malignant meningioma with verotoxin. Neoplasia. 2002;4(4):304–11.
35. Johansson D, Johansson A, Grankvist K, Andersson U, Henriksson R, Bergström P, et al. Verotoxin-1 induction of apoptosis in Gb3-expressing human glioma cell lines. Cancer Biol Ther [Internet]. 2006 Sep [cited 2020 May 2];5(9):1211–7. Available from: http://www.ncbi.nlm.nih.gov/pubmed/16929170
36. Nudelman E, Kannagi R, Hakomori S, Parsons M, Lipinski M, Wiels J, et al. A glycolipid antigen associated with burkitt lymphoma defined by a monoclonal antibody. Science (80-). 1983;220(4596):509–11.
37. Ito M, Suzuki E, Naiki M, Sendo F, Arai S. Carbohydrates as antigenic determinants of tumor-associated antigens recognized by monoclonal anti-tumor antibodies produced in a syngeneic system. Int J Cancer. 1984;34(5):689–97.
38. Kovbasnjuk O, Mourtazina R, Baibakov B, Wang T, Elowsky C, Choti MA, et al. The glycosphingolipid globotriaosylceramide in the metastatic transformation of colon cancer. Proc Natl Acad Sci U S A. 2005 Dec 27;102(52):19087–92.
39. Xu H, Peng L, Shen M, Xia Y, Li Z, He N. Shiga-like toxin I exerts specific and potent anti-tumour efficacy against gastric cancer cell proliferation when driven by tumour-preferential Frizzled-7 promoter. Cell Prolif. 2019 May 1;52(3).
40. Iturrioz-Rodríguez N, Correa-Duarte MA, Fanarraga ML. Controlled drug delivery systems for cancer based on mesoporous silica nanoparticles. Vol. 14, International Journal of Nanomedicine. Dove Medical Press Ltd.; 2019. p. 3389–401.
41. Lu F, Wu SH, Hung Y, Mou CY. Size effect on cell uptake in well-suspended, uniform mesoporous silica nanoparticles. Small [Internet]. 2009 Jun 19 [cited 2020 May 2];5(12):1408–13. Available from: http://doi.wiley.com/10.1002/smll.200900005
42. Narayan R, Nayak UY, Raichur AM, Garg S. Mesoporous silica nanoparticles: A

comprehensive review on synthesis and recent advances. Vol. 10, Pharmaceutics. MDPI AG; 2018.
43. Kim IY, Joachim E, Choi H, Kim K. Toxicity of silica nanoparticles depends on size, dose, and cell type. Nanomedicine Nanotechnology, Biol Med. 2015 Aug 1;11(6):1407–16.
44. Yang SA, Choi S, Jeon SM, Yu J. Silica nanoparticle stability in biological media revisited. Sci Rep [Internet]. 2018;8(1):1–9. Available from: http://dx.doi.org/10.1038/s41598-017-18502-8
45. Arvizo RR, Miranda OR, Moyano DF, Walden CA, Giri K, Bhattacharya R, et al. Modulating pharmacokinetics, tumor uptake and biodistribution by engineered nanoparticles. PLoS One. 2011 Sep 13;6(9).
46. Liu L, Hitchens TK, Ye Q, Wu Y, Barbe B, Prior DE, et al. Decreased reticuloendothelial system clearance and increased blood half-life and immune cell labeling for nano- and micron-sized superparamagnetic iron-oxide particles upon pre-treatment with Intralipid. Biochim Biophys Acta - Gen Subj. 2013 Jun;1830(6):3447–53.
47. Luchini A, Vitiello G. Understanding the nano-bio interfaces: Lipid-coatings for inorganic nanoparticles as promising strategy for biomedical applications. Vol. 7, Frontiers in Chemistry. Frontiers Media S.A.; 2019.
48. Blanco E, Shen H, Ferrari M. Principles of nanoparticle design for overcoming biological barriers to drug delivery. Vol. 33, Nature Biotechnology. Nature Publishing Group; 2015. p. 941–51.
49. Mroz EA, Rocco JW. Intra-tumor heterogeneity in head and neck cancer and its clinical implications. World J Otorhinolaryngol Neck Surg. 2016 Jun;2(2):60–7.
50. Wang M, Zhao J, Zhang L, Wei F, Lian Y, Wu Y, et al. Role of tumor microenvironment in tumorigenesis. Vol. 8, Journal of Cancer. Ivyspring International Publisher; 2017. p. 761–73.
51. Roma-Rodrigues C, Mendes R, Baptista P V., Fernandes AR. Targeting tumor microenvironment for cancer therapy. Vol. 20, International Journal of Molecular Sciences. MDPI AG; 2019.
52. Pickup MW, Mouw JK, Weaver VM. The extracellular matrix modulates the hallmarks of cancer. EMBO Rep. 2014 Dec;15(12):1243–53.
53. Otranto M, Sarrazy V, Bonté F, Hinz B, Gabbiani G, Desmoulière A. The role of the myofibroblast in tumor stroma remodeling. Vol. 6, Cell Adhesion and Migration. Taylor and Francis Inc.; 2012. p. 203–19.
54. Ziello JE, Jovin IS, Huang Y. Hypoxia-Inducible Factor (HIF)-1 regulatory pathway and its potential for therapeutic intervention in malignancy and ischemia. Vol. 80, Yale Journal of Biology and Medicine. Yale Journal of Biology and Medicine; 2007. p. 51–60.
55. Klein D. The tumor vascular endothelium as decision maker in cancer therapy. Vol. 8, Frontiers in Oncology. Frontiers Media S.A.; 2018.
56. Navarro Palomares EM, Barroso Valiente R, Villegas Sordo JC. Desarrollo de nanopartículas. Cantabria; 2019.
57. Hakomori S-I. Bifunctional role of glycosphingolipids. J Biol Chem. 1990;265(November 5):18713–6.
58. Trofa AF, Ueno-Olsen H, Oiwa R, Yoshikawa M. Dr. Kiyoshi Shiga: Discoverer of the Dysentery Bacillus. Clin Infect Dis. 1999;29(5):1303–6.

59. Engedal N, Skotland T, Torgersen ML, Sandvig K. Shiga toxin and its use in targeted cancer therapy and imaging. Vol. 4, Microbial Biotechnology. Wiley-Blackwell; 2011. p. 32–46.
60. Rípodas Navarro A, Fernández Moreira D, Macho Martínez M. Investigación de Escherichia Coli productor de toxinas Shiga (STEC) en carnes y derivados cárnicos. Sanid Mil. 2017;73(3):147–52.
61. Melton-Celsa AR. Shiga Toxin (Stx) Classification, Structure, and Function. Microbiol Spectr. 2014 Aug 22;2(4).
62. Katagiri YU, Mori T, Nakajima H, Katagiri C, Taguchi T, Takeda T, et al. Activation of Src family kinase Yes induced by shiga toxin binding to globotriaosyl ceramide (Gb3/CD77) in low density, detergent-insoluble microdomains. J Biol Chem. 1999 Dec 3;274(49):35278–82.
63. Sandvig K, Bergan J, Dyve AB, Skotland T, Torgersen ML. Endocytosis and retrograde transport of Shiga toxin. Vol. 56, Toxicon. Pergamon; 2010. p. 1181–5.
64. Garred O, Van Deurs B, Sandvig K. Furin-induced cleavage and activation of shiga toxin. J Biol Chem. 1995 May 5;270(18):10817–21.
65. He Q, Shi J. Mesoporous silica nanoparticle based nano drug delivery systems: Synthesis, controlled drug release and delivery, pharmacokinetics and biocompatibility. J Mater Chem. 2011 Apr 28;21(16):5845–55.
66. García J, Santana Z, Zumalacárregui L, Quintana M, González D, Furrazola G, et al. Estrategias de obtención de proteínas recombinantes en escherichia coli. Vaccimonitor. 2013;22(2):30–9.
67. Zimmer M. GFP: From jellyfish to the Nobel prize and beyond. Chem Soc Rev. 2009;38(10):2823–32.
68. Garritz A. Shimomura, Chalfie y Tsien: los señores de la proteína verde bioluminiscente de la medusa Aequorea victoria. Educ Química. 2009 Jan 1;20(1):75–6.
69. Melton-Celsa AR, O'Brien AD. Shiga Toxins of Shigella dysenteriae and Escherichia coli. In: Bacterial Protein Toxins. Springer Berlin Heidelberg; 2000. p. 385–406.
70. Cuadros-Rodríguez L, Bagur-González MG, Sánchez-Viñas M, González-Casado A, Gómez-Sáez AM. Principles of analytical calibration/quantification for the separation sciences. J Chromatogr A. 2007;1158(1–2):33–46.
71. Harris D. Análisis químico cuantitativo - Daniel C. Harris - Google Libros. In: Análisis químico cuantitativo [Internet]. 2007 [cited 2020 May 2]. p. 315. Available from: https://books.google.es/books?id=H-_8vZYdL70C&pg=PR3&dq=Quantitative+chemical+analysis.+Daniel+C.+Harris.+Ed.+Reverté.+3º+Edition.&hl=es&sa=X&ved=0ahUKEwjE-JnzuZXpAhWl4IUKHfVvC60Q6AEIOzAC#v=onepage&q=Quantitative chemical analysis. Daniel C. Harris. Ed. R
72. Áncer COELC. Bioquímica de los Taxoides Utilizados Contra el Cáncer (B t u c c). 2011;30(1):12–20.

Acknowledgments

I have always considered time as one of the most valuable possessions we have as living beings and even more so as human beings, since we can choose how and with whom to spend the time we have. For this reason I want to thank my tutors Mónica and Nerea for their time, their dedication and for all the support they have given me to do this work.

I also want to thank Marisa Maliaño Toca for encouraging me to study medicine and helping me to embark on this adventure and for believing in me even in moments when not even I trusted.

I want to thank my friends Benedetta, Annick, Lydia, Manu ... and many others without whom it would not have been so much fun to study this degree. Thanks for the laughter and the tears, the memories, the wear ...

And finally to my family who always believed in me and who taught me something very important and that today I am proud to say: that I have learned that it does not matter how many times life hits you and knocks you down, but what matters really is the times you can find the strength to get up and start again. And that distances do not matter because they will always be by my side even if we are separated by so many kilometers of sea.